Supporting Information

Intrinsic Limits of Defect-State Photoluminescence Dynamics in Functionalized Carbon Nanotubes

Xiaowei He[1], Liuyang Sun[2], Brendan Gifford[3,4], Sergei Tretiak[1,3], Andrei Piryatinski[3], Xiaoqin Li[2], Han Htoon[1,*], Stephen K. Doorn[1,*]

[1]Center for Integrated Nanotechnologies, Materials Physics and Applications Division, Los Alamos National Laboratory, Los Alamos, New Mexico 87545, United States

[2]Department of Physics, University of Texas-Austin, Austin, Texas 78712, United States

[3]Theoretical Division, Los Alamos National Laboratory, Los Alamos, New Mexico 87545, United States

[4]Center for Nonlinear Sciences, Los Alamos National Laboratory, Los Alamos, New Mexico 87545, United States

I. Time-Dependent Density Functional Theory (TD-DFT) Radiative Rate Calculation

Our simulations use a well-established modeling approach using DFT and TD-DFT techniques applied to long segments of functionalized SWCNTs that have been properly capped on the ends.[1-4] Namely, pristine (6,5) single-wall carbon nanotubes of ~12 nm (generated from 3 unit-cells) in length were generated using VMD 1.9.3 software.[5] Where finite computational systems are required, SWCNTs must first be capped at their ends in order to replicate the electronic structure of respective infinite-length systems. The capping scheme used here utilizes hydrogen atoms at every terminal carbon atom, as has been previously demonstrated to be the appropriate capping scheme for (6,5) chirality systems.[1,2] The systems were then functionalized with aryl-based functional groups located approximately at the center of the SWCNT. The functionalization schemes generated are presented in a previous report.[3] To avoid the formation of open-shell systems, a second hydrogen was used to bind the remaining reactive electron. This atom was placed in positions either adjacent to the functional group (ortho) or across the hexagonal ring from the functional group (para) as have previously been described as topologically relevant positions.[3,4]

TD-DFT was then used to optimize excited state geometries of each system using the CAM-B3LYP density functional, as has been previously shown to reasonably determine electron localization in functionalized SWCNT systems[6] and reasonably agrees with experiments.[7,8] Since relative trends of lifetimes are of interest for this study and optical energies in these systems have been previously shown to be independent of basis set size,[3] the minimal STO-3G basis set[9] was used. Here we use the Gaussian09 software package[10] for all simulations. These quantum-chemical simulations yield the optical transition energies and intensities (oscillator

strengths) required for subsequent evaluation of radiative lifetimes using the following equation:

$$\tau = \frac{2\pi c^3 \varepsilon_0 m_e}{f\omega^2 e^2} \quad \text{(Eq. 1)}$$

where c is the speed of light, ε_0 is the vacuum permittivity, m_e is the mass of an electron, e is the elementary charge, and f and ω are the oscillator strength and angular frequency of the lowest excited state transition, respectively, calculated with TD-DFT. The oscillator strength is related to the transition dipoles through the following expression:

$$f = \frac{2\omega m_e}{3e^2\hbar} D^2 \quad \text{(Eq. 2)}$$

where D is the transition dipole from the TD-DFT calculation and all other parameters have been previously defined. This approach is very similar to one previously followed for estimating lifetimes.[11,12] In this case, energies corrected to match experiment based on our previously defined model[13] were used. We note that para configurations are typically not observed, or are observed very weakly in experimental spectra.[14] Of the ortho configurations, L_{90} has previously been identified as the state corresponding to the E_{11}* emission band,[3,4,14] thus the relevant radiative lifetime for comparison to the main text discussion is 2.12 ns (Table S1).

Configuration		E_{emis} (eV, as calculated)	E_{emis} (eV, corrected)	Emission Transition Dipole (Debye)	Lifetime from calculated energies (ns)	Lifetime from Corrected Energies (ns)
Pristine		1.95	1.25	67.4	0.18	0.44
Ortho	L_{30}	1.40	0.93	36.2	1.68	3.85
	L_{90}	1.65	1.08	38.7	0.90	2.12
	L_{-30}	1.89	1.22	40.2	0.56	1.34
Para	L_{30}	1.92	1.23	38.1	0.59	1.43
	L_{90}	1.53	1.00	37.0	1.25	2.90
	L_{-30}	1.34	0.89	36.6	1.88	4.28

Table S1: TD-DFT results for aryl-functionalized (6,5) SWCNTs, including energies of emission, corrected emission,[13] transition dipoles and radiative lifetimes calculated from both transition energies.

II. Biexponential PL Decay

In agreement with previous work,[15] we find that defect-state PL decays may be fit to a biexponential (see Fig. 4a main text). It has been shown previously that the biexponential decay is a consequence of the existence of a dark defect state that lies ~ 10 meV higher in energy above the emitting defect state (for sp^3 defects).[16] The long decay component (τ_L) has been shown to correspond to the rate of overall loss of population from the defect-state manifold (dark plus bright emitting state), while the short component (τ_S) has been established as the time constant for exchange of population between the bright and dark defect states.[15,17] Values of the fitting parameters τ_L and τ_S and the corresponding prefactors A_L and A_S are given in Tables S1 and S2 for the lifetime data shown in the main text Figs. 4b and 6b, respectively.

Table S1. Biexponential fitting parameters for PL lifetime data of Fig. 4b, main text.

	τ_l value (ns)	A_l weight (%)	τ_s value (ns)	A_s weight (%)
1120	1.39	88.5	0.094	11.5
1124	1.5	87.7	0.058	12.3
1131	1.17	89.2	0.067	10.8
1137	1.36	88.8	0.085	11.2
1139	1.258	90.5	0.125	9.5
1142	1.33	92.2	0.094	7.8
1150	1.214	89.9	0.091	10.1
1155	1.127	93.4	0.145	6.6
1165	1.212	87.6	0.097	12.4
1170	0.994	91.1	0.115	8.9
1182	0.958	88.6	0.084	11.4
1186	1.143	95.1	0.172	1.9
1195	1.162	92.2	0.104	7.8
1201	0.986	90.9	0.101	9.1
1210	1.01	89	0.194	11
1225	0.947	95.5	0.125	4.5
1240	1.035	93.4	0.117	6.6
1257	0.979	96.1	0.191	3.9
1265	1.08	95.2	0.109	4.8
1268	0.952	94.5	0.187	5.5
1278	0.934	93.2	0.198	6.8

Table S2. Biexponential fitting parameters for PL lifetime data of Fig. 6b, main text.

	τ_l value (ns)	A_l weight (%)	τ_s value (ns)	A_s weight (%)
1119	1.21	89.5	0.068	10.5
1125	1.38	86.6	0.095	13.4
1139	1.19	92.4	0.081	7.6
1157	0.934	95.5	0.095	4.5
1165	0.924	89.5	0.125	10.5
1248	0.875	94.2	0.107	5.8
1276	0.965	95.1	0.118	4.9

III. Spectral Diffusion over Long Observation Times.

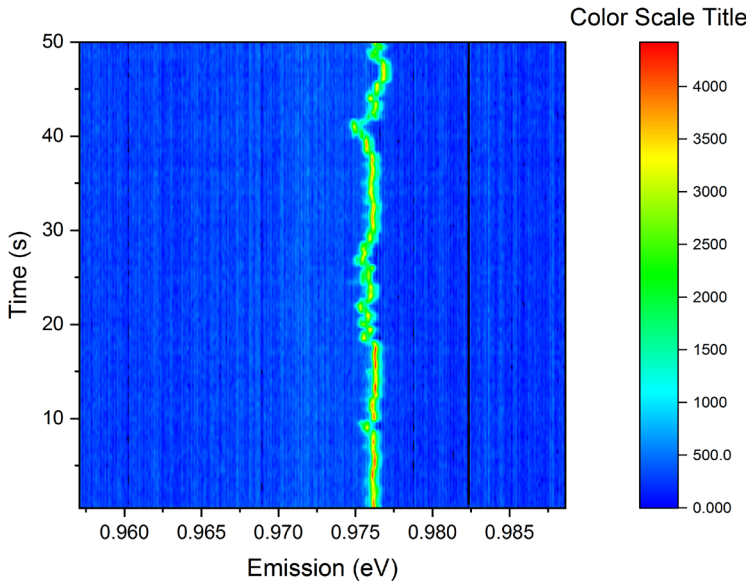

Fig. S1. E11* photoluminescence spectral wandering tracked over 1 minute of measurement time. Each spectrum is integrated for 0.5 seconds. While individual linewidths are ~ 0.25 meV, spectral variation across all spectra occurs in the range of +/- 0.8 meV. Data measured at 4K.

References:

(1) S. Kilina and S. Tretiak, *Adv. Funct. Mater.,* 2007, **17**, 3405–3420.
(2) A. Sharma, B. J. Gifford and S. Kilina, *J. Phys. Chem. C,* 2017, **121**, 8601–8612.
(3) B. J. Gifford, S. V. Kilina, H. Htoon, S. K. Doorn and S. Tretiak, *J. Phys. Chem. C,* 2018**,** **122**, 1828-1838.
(4) X. He, B. J. Gifford, N. F. Hartmann, R. Ihly, X. Ma, S. V. Kilina, Y. Luo, K. Shayan, S. Strauf, J. L. Blackburn, S. Tretiak, S. K. Doorn and H. Htoon, *ACS Nano,* 2017, **11**, 10785–10796.
(5) W. Humphrey, A. Dalkeand K. Schulten, *J. Mol. Graph.,* 1996, **14**, 33–38.
(6) L. Adamska, G. V. Nazin, S. K. Doorn and S. Tretiak, *J. Phys. Chem. Lett.,* 2015, **6**, 3873–3879.
(7) S. Kilina, E. Badaeva, A. Piryatinski, S. Tretiak, A. Saxena and A. R. Bishop, *Phys. Chem. Chem. Phys.,* 2009, **11**, 4113–4123.
(8) S. Kilina, D. Kilin and S. Tretiak, *Chem. Rev.,* 2015, **115**, 5929–5978.
(9) W. J. Hehre, R. F. Stewart and J. A. Pople, *J. Chem. Phys.* 1969, **51**, 2657–2664.
(10) M. J. Frisch, G. W. Trucks, H. B. Schlegel, G. E. Scuseria, M. A. Robb, J. R. Cheeseman, G. Scalmani, V. Barone, B. Mennucci, G. A. Petersson, *Gaussian 09*; Gaussian, Inc.: Wallingford, CT, USA, 2009.
(11) J. Chen, A. Schmitz and D. S. Kilin, *Int. J. Quantum Chem.,* 2012, **112**, 3879–3888.
(12) S. Kilina, J. Ramirez and S. Tretiak, *Nano Lett.,* 2012, **12**, 2306–2312.
(13) B. J. Gifford, A. E. Sifain, H. Htoon, S. K. Doorn, S. Kilina and Tretiak, *J. Phys. Chem. Lett.,* 2018, **9**, 2460–2468.
(14) A. Saha, B. J. Gifford, X. He, G. Ao, M. Zheng, H. Kataura, H. Htoon, S. Kilina, S. Tretiak and S. K. Doorn, *Nat. Chem.,* 2018, **10**, 1089-1095.
(15) N. F. Hartmann, K. A. Velizhanin, E. H. Haroz, M. Kim, X. Ma, Y. Wang, H. Htoon and S. K. Doorn, *ACS Nano,* 2016, **10**, 8355-8365.
(16) M. Kim, L. Adamska, N. F. Hartmann, H. Kwon, J. Liu, K. A. Velizhanin, Y. Piao, L. R. Powell, B. Meany, S. K. Doorn, S. Tretiak and Y. Wang, *J. Phys. Chem. C*, 2016, **120**, 11268-11276.
(17) X. He, K. A. Velizhanin, G. Bullard, Y. Bai, J.-H. Olivier, N. F. Hartmann, B. J. Gifford, S. Kilina, S. Tretiak, H. Htoon, M. J. Therien and S. K. Doorn, *ACS Nano,* 2018, **12**, 8060-8070.